Available online at www.sciencedirect.com
ScienceDirect
Journal of Photochemistry and Photobiology A: Chemistry 189 (2007) 39–45
Journal of Photochemistry and Photobiology A:Chemistry
www.elsevier.com/locate/jphotochem

Luminescence and Raman spectroscopic studies on the damage of tryptophan, histidine and carnosine by singlet oxygen

Chunying Wei [a], Bo Song [b], Jingli Yuan [b], Zhaochi Feng [a], Guoqing Jia [a], Can Li [a,*]

[a] *State Key Laboratory of Catalysis, Dalian Institute of Chemical Physics, Chinese Academy of Sciences, Dalian 116023, China*
[b] *Laboratory of Analytical Chemistry, Dalian Institute of Chemical Physics, Chinese Academy of Sciences, Dalian 116023, China*

Received 29 September 2006; received in revised form 13 December 2006; accepted 10 January 2007
Available online 16 January 2007

Abstract

In connection with the chemical modification of protein, the photooxidation of histidine (His), tryptophan (Trp) and carnosine by singlet oxygen ($^1O_2$) is investigated by a Eu^{3+} luminescence probe ATTA-Eu^{3+} and UV Raman spectroscopy under physiological conditions (pH 7.5). The solutions containing both the luminescence probe ATTA-Eu^{3+}(1×10^{-5} M) and the different concentration of the biological targets His, Trp or carnosine were irradiated by a tungsten lamp in the presence of $^1O_2$ photosensitizer H_2TMPyP4 (1×10^{-5} M), the luminescence intensity of the Eu^{3+} complex probe decreases linearly with increasing the concentration of the biological target. The reaction rate constants of $^1O_2$ with His, Trp and carnosine were calculated to be 3.2×10^8, 7.7×10^7 and 1.3×10^8 M^{-1} s^{-1}, respectively. The results suggest that the luminescence probe ATTA-Eu^{3+} can be used for detecting the reactions of $^1O_2$ with the biological targets quantitatively under physiological conditions. UV Raman spectroscopy probes the structural changes of these biological targets after reaction with $^1O_2$, indicating that peroxides are main species for the reaction of Trp although the products decomposed by peroxides are main forms for that of His in a buffer solution. The imidazole ring of carnosine is the target of $^1O_2$, and the peptide bond is almost intact after reaction with $^1O_2$.

Keywords: Singlet oxygen; Carnosine; Amino acids; Spectroscopy

1. Introduction

The molecular oxygen in the lowest excited electronic state, singlet molecular oxygen ($^1O_2$), is a highly reactive oxidant for biological system. It can be readily produced upon irradiation of a photosensitizer that transfers its excited state energy to ground-stated dioxygen ($^3O_2$), and also by some enzymatic reactions catalyzed by peroxidases or oxygenases in biological systems [1]. Singlet oxygen can react rapidly with many biological molecules, such as DNA, RNA, lipids, sterols, free amino acids, peptides and proteins [2–4]. Due to the abundance of proteins within most biological systems and the high reaction rate constants for the reaction of $^1O_2$ with some protein side-chains, proteins and some amino acids are the major targets for $^1O_2$ [5]. It is known that many products of such oxidation are poorly repaired, peroxides generated on peptides and proteins by $^1O_2$ are relatively easy to react with antioxidants, such as the low molecular mass thiols and proteins containing thiol groups, to modify the prosthetic group within the protein structure [6] even to induce DNA base oxidation, strand breaks, DNA-protein cross-links oxidation [7]. These modified species can result in wide-ranging biophysical and biochemical changes in both the properties and functions of cells, and may be key intermediates in cellular dysfunction and disease progress [6,7].

Among the amino acids, both tryptophan (Trp) and histidine (His) can react with $^1O_2$ at significant rates under physiological pH condition. The majority of reactions of $^1O_2$ with His and Trp occur via the chemical routes that will result in modification of the target, while Trp also gives significant physical quenching [8]. Carnosine, a biologically important dipeptide, is a histidine-containing dipeptide that is present in relatively high concentrations (1–20 mM) in several mammalian tissues, such as skeletal muscle and brain. Carnosine has an excellent potential to act as a natural antioxidant in vivo, in fact, it is an efficient $^1O_2$ scavenger [9].

* Corresponding author. Tel.: +86 411 84379070; fax: +86 411 84694447.
E-mail address: canli@dicp.ac.cn (C. Li).
URL: http://www.canli.dicp.ac.cn.

1010-6030/$ – see front matter © 2007 Elsevier B.V. All rights reserved.
doi:10.1016/j.jphotochem.2007.01.005

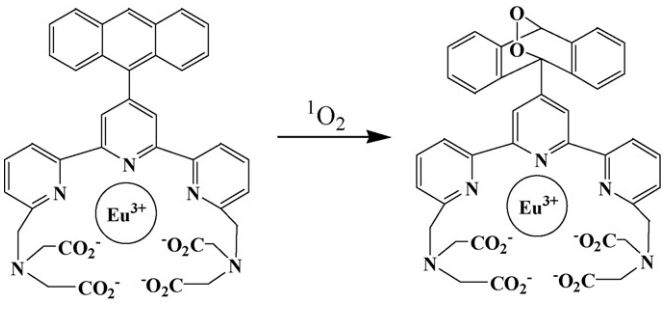

Scheme 1. Reaction of ATTA-Eu^{3+} with $^1O_2$.

The deleterious effects of $^1O_2$ in biological systems have received increasing recognition recently. A number of methods for $^1O_2$ detection have been developed. For example, $^1O_2$ can be directly detected by monitoring its emission at 1270 nm [1,10] and by chemical trapping with some spectroscopic probes [11]. Recently, Song et al. developed a Eu^{3+} complex, [4′-(9-anthryl)-2,2′:6′,2″-terpyridine-6,6″diyl]bis(methylenenitrilo) tetrakis(acetate)-Eu^{3+} (ATTA-Eu^{3+}), that can be used as a sensitive and specific luminescence probe for $^1O_2$ in a weakly basic, neutral or weakly acidic buffer [12,13]. This Eu^{3+} complex is nearly non-luminescent, and can specifically react with $^1O_2$ to form a highly luminescent endoperoxide (Ep-ATTA-Eu^{3+}, Scheme 1) with a long luminescence lifetime. Herein, we report the application of this probe in detecting the reaction of $^1O_2$ with three biological target molecules Trp, His and carnosine under physiological pH condition.

On the other hand, the chemical quenching of $^1O_2$ can result in the modification of the targets to yield complicated products. These species have major effects on the cellular function. However, to our knowledge, there have been much less work reported on the detailed spectroscopic investigation on target modification. So another aim of this study is to investigate the structural changes after the reactions of $^1O_2$ with Trp, His and carnosine under physiological pH condition by UV Raman spectroscopy.

In the present work, we found that the ATTA-Eu^{3+} complex can probe the reactions of $^1O_2$ with the biological target molecules Trp, His and carnosine under physiological pH condition, and gives their reaction rate constants quantitatively. Furthermore, the information of structural changes for the $^1O_2$-promoted oxidation of His, Trp and carnosine was obtained by UV Raman spectroscopy. The results also provide the useful insights into the damage mechanisms of amino acids and even proteins by $^1O_2$.

2. Materials and methods

2.1. Chemicals

L-Tryptophan (Trp) and L-histidine (His) were purchased from Shanghai Chemical Reagent Company (China) and were used without further purification. Carnosine (β-alanyl-L-histidine) was purchased form Sigma–Aldrich. H_2TMPyP4 (5,10,15,20-tetrakis (1-methy-4-pyridyl)-21H, 23H-porphine) was purchased in the form of tetra-p-tosylate salt from Tokyo Kasei Kogyo Co., Ltd. (Japan). [4′-(9-Anthryl)-2,2′:6′,2″-terpyridine-6,6″-diyl]bis(methylenenitrilo)tetrakis(acetate)-Eu^{3+} (ATTA-Eu^{3+}) were synthesized according to a literature method [12].

2.2. Time-resolved luminescence measurement

The time-resolved luminescence measurement was carried out on a Perkin-Elmer Victor 1420 multilabel counter with the excitation wavelength, 340 nm; emission wavelength, 615 nm; delay time, 0.2 ms; window time (counting time), 0.4 ms; cycling time, 1.0 ms.

The reaction rate constants of Trp, His and carnosine with $^1O_2$ were determined by a fluorometric method using the competitive reaction between ATTA-Eu^{3+} and the amino acid (or carnosine) with $^1O_2$ produced by the irradiation of H_2TMPyP4 in an oxygen-saturated buffer solution. The reaction rate constants of Trp, His and carnosine with $^1O_2$ were calculated according to Eq. (1), where I_0/I is the ratio of the luminescence intensity of the Eu^{3+} complex in the absence and presence of the amino acid (or carnosine), k_T is the rate constant for ATTA-Eu^{3+}-$^1O_2$ reaction, k_d is the decay rate of $^1O_2$ in an aqueous solution, k_q is the rate constant for Trp, His or carnosine-$^1O_2$ reaction, T is the concentration of ATTA-Eu^{3+} and Q is the concentration of the amino acid (or carnosine) [14,15].

$$\frac{I_0}{I} = 1 + \frac{k_q}{k_T[T] + k_d}[Q] \quad (1)$$

The photosensitization reactions were carried out in oxygen-saturated 50 mM Tris–HCl buffer at pH 7.4. The buffer solution containing 10 μM TMPyP4, 10 μM ATTA-Eu^{3+} and different concentrations of either the amino acid or carnosine (from 0 to 3 mM) were irradiated by a 100 W tungsten lamp for 20 min. After the reaction, the solution was 100-fold diluted (the final probe concentration is 100 nM) with buffer solution, and subjected to time-resolved luminescence measurement on a Perkin-Elmer Victor 1420 Multilable Counter at room temperature.

2.3. UV Raman spectroscopy

UV Raman spectroscopy was carried out on a home built instrument with T64000 triple-stage spectrometer of Jobin Yvon S.A. equipped with three gratings and a specially coated UV-sensitive CCD detector. A 244 nm line from a Coherent Innova 300 FRED laser was used as the excitation source. The spectra were recorded using a 90° geometry with a laser power of less than 1 mW on the sample to avoid the damage of the sample. Each spectrum was collected for 60 s; two spectra were accumulated to increase the signal-to-noise ratio. No photochemical damage was observed for all samples as judged by the absence of transient and irreversible changes in UV Raman spectra within the time of datum collection. Raman frequencies were calibrated using the spectrum of Teflon.

The buffer solutions of Trp, His and carnosine containing 10 μM TMPyP4 were irradiated by a 100 W tungsten lamp for

25, 50 and 75 min, respectively. After the irradiation, the solution temperature is a little high compared with the room temperature. In order to avoid the effect of the solution temperature on the Raman spectra, the solution was cooled to room temperature after the reaction, and then UV Raman spectra were taken immediately. The concentrations of Trp, His and carnosine were fixed at 1.0×10^{-3}, 1×10^{-2} and 5×10^{-2} M, respectively, in buffer solutions containing 50 mM Tris–HCl, 150 mM $NaClO_4$ (pH 7.5). The Raman band at 933 cm^{-1} of $NaClO_4$ in buffer solution was chosen as the intensity internal standard.

3. Results and discussion

3.1. Measurement of reaction rate constants of Trp, His and carnosine with $^1O_2$ by the luminescence probe

Indole ring of Trp and imidazole rings of His and carnosine are easy to react with $^1O_2$ and have shown to be responsible for antioxidation activity in vivo [16–18]. The ATTA-Eu^{3+} complex can specifically react with $^1O_2$ accompanied by the remarkable luminescence increase upon the reaction [12,13]. In order to examine whether the ATTA-Eu^{3+} complex can probe the reaction of $^1O_2$ with the biological targets under physiological pH condition, we determined the effects of different concentrations of Trp, His and carnosine on the luminescence intensities of the Eu^{3+} complex after the solutions were irradiated by visible light for 20 min in the presence of $^1O_2$ photosensitizer H_2TMPyP4. As shown in Fig. 1, the luminescence intensity of the product of ATTA-Eu^{3+} reacted with $^1O_2$ was decreased significantly with the increase of the concentrations of Trp, His and carnosine, and the effects of these target molecules on the luminescence intensity were found in the order of Trp > carnosine > His. These results indicate that the ATTA-Eu^{3+} complex can probe the reactions of $^1O_2$ with Trp, His and carnosine under physiological pH condition.

As shown in Table 1, the reaction rate constants of Trp, His and carnosine with $^1O_2$ were calculated to be 3.2×10^8, 7.7×10^7 and 1.3×10^8 M^{-1} s^{-1} by Eq. (1), respectively, using $k_T = 3.3 \times 10^9$ M^{-1} s^{-1} [19] and $k_d = 2.38 \times 10^5$ s^{-1} [20]. The results of this method show a consistency with the reported values [2,18], especially for His and carnosine, which indicates that the ATTA-Eu^{3+} complex can be used to quantitatively detect the reactions of $^1O_2$ with amino acids and small peptides. It has been reported that the chemical rate constant for L-histidine-$^1O_2$ is in the range of 4×10^7 to 1×10^8 M^{-1} s^{-1} [21,22], and carnosine containing the imidazole ring is a more effective $^1O_2$ scavenger than L-histidine in aqueous solutions and in biological system [16,23]. Our results are in good agreement with this conclusion.

Table 1
Comparison of the quenching rate constant (k_q) for the reaction of $^1O_2$ with Trp, His and carnosine using ATTA-Eu^{3+} probe[a] with literature results[b,c]

Compounds	k_q (M^{-1} s^{-1})[a]	k_q (M^{-1} s^{-1})[b,c]
Trp	3.2×10^8	1.0×10^8[b], 4.0×10^7[c]
His	7.7×10^7	3.2×10^7[b], 5.0×10^7[c]
Carnosine	1.3×10^8	–

[a] This work.
[b] Value according to Ref. [2].
[c] Value according to Ref. [18].

In the case of Trp, it was found that a broad absorption band around 340 nm was formed after the irradiation, and the maximum absorption band of TMPyP4 was shifted from 424 to 476 nm (data not shown), which indicate that some new colored species were produced upon the irradiation. Because these colored species can absorb the incident and emission lights, resulting in the decrease of the I value in Eq. (1) due to the luminescence internal filter effect, the rate constant obtained for Trp is a little high compared with literature values and the intercept in the Stern–Volmer plot does not have an intercept of unity. In fact, the structure changes of Trp, His and carnosine after they

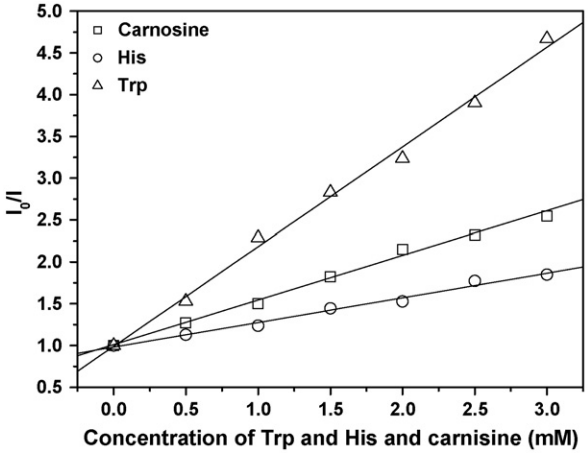

Fig. 1. Stern–Volmer plots of the luminescence intensity of the Eu^{3+} complex against the concentrations of Trp, His and carnosine.

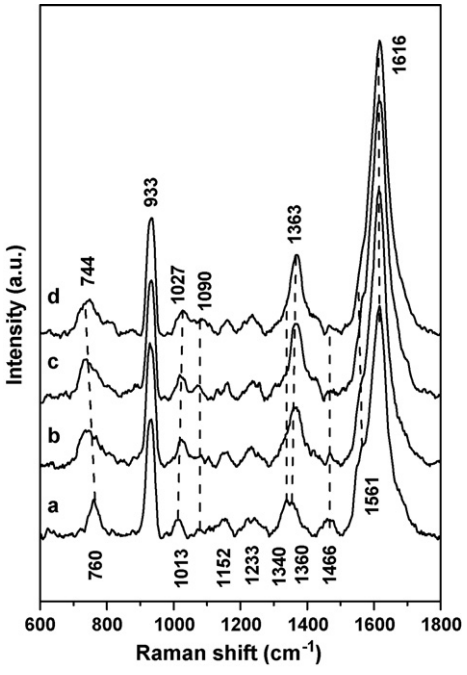

Fig. 2. UV resonance Raman spectra of Trp at 1.0×10^{-3} M before irradiation (a), after irradiation for 20 min (b), 50 min (c) and 75 min (d) in buffer solution containing 50 mM Tris–HCl, 120 mM $NaClO_4$ (pH 7.5).

react with $^1O_2$ are very significant and some new species are produced in the solution (see below), so other quenching reactions may also occur in these complex systems.

3.2. Structural characterization of Trp, His and carnosine reaction with $^1O_2$ by UV Raman spectroscopy

Raman spectroscopy is a powerful tool for structural characterization of molecules. UV Raman spectroscopy can enhance the Raman intensities of the bands of molecules at relatively low concentration and is suitable to detect the structural changes of biological molecules [24]. In order to investigate the $^1O_2$-induced the structural damages of Trp, His and carnosine, we carried out UV Raman studies on the reactions of Trp, His and carnosine with $^1O_2$ using a 244 nm line. In this case, UV resonance Raman spectra are obtained for Trp because the 244 nm line is in the range of its absorption band [25].

Fig. 2 shows UV resonance Raman spectra of 1×10^{-3} M Trp before and after irradiation for 25, 50 and 75 min in the presence of 10^{-5} M TMPyP4 in a neutral buffer solution. The characteristic Raman band of ClO_4^- (933 cm^{-1}) was used as an internal standard band to normalize the intensity of the Raman spectra. The Raman signal was not observed for 10^{-5} M TMPyP4 when excited by a 244 nm laser (data not shown). UV resonance Raman bands of Trp and their assignments are summarized in Table 2.

Compared with the reaction taken before the irradiation, almost all bands are shifted with large intensity changes after the irradiation in the presence of TMPyP4, suggesting that the structural modification of $^1O_2$ to Trp is significant. According to the assignments of bands in Table 2, the resonance Raman bands of Trp when excited by 244 nm laser are all related to the vibrations of indole ring. The bands at 760 and 1013 cm^{-1}, ascribed to the ring breathing modes of pyrrole and benzene [26], are broadened and shifted to 744 and 1027 cm^{-1}, respectively. In addition, a new weak broad band near 1090 cm^{-1} is ascribed to the stretching vibration of the O–O bond in O_2^- [27], which indicates that $^1O_2$ reacts with Trp to produce the peroxide species.

The bands at 1340 and 1360 cm^{-1} are shifted to the 1363 cm^{-1} and appear as a singlet, with almost two-fold increased intensity. The bands at 1360/1340 cm^{-1}, a Fermi doublet between a fundamental band of an in-plane vibration (mainly N1-C8 stretch) and one or more combination band of out-of-plane vibrations involving the benzene and pyrrole rings,

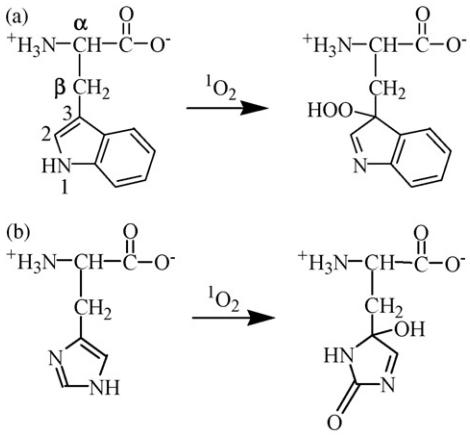

Scheme 2. Reaction of Trp (a) and His (b) with $^1O_2$.

are sensitive to the change of the hydrophobic environment of indole ring, the stronger the hydrophobicity the higher intensity ratio of doublet (I_{1360}/I_{1340}) [28–30]. On the contrary, the band at 1466 cm^{-1}, corresponding to the NH bending vibration of the indole [30,31], disappears, which indicates that H atom of N–H bond is transferred after the reaction of Trp with $^1O_2$. The intensity of the band at 1616 cm^{-1}, assigned to the stretching vibration of C=C bond, is increased with irradiation. The band at 1561 cm^{-1} arises from indole ring vibration mainly contributed from the C2=C3 stretching. Because of its vibration mode, the shift of this band is expected to be affected by the torsion angle about the C_α–C_β–C3=C2 linkage [29,30]. The curve fitting indicates that the band at 1561 cm^{-1} is shifted to 1585 cm^{-1} and buried in the band of 1616 cm^{-1}, and its intensity is also decreased. According to the changes of Raman spectra and the results about the damage of $^1O_2$ to Trp reported by the literatures, the reaction between Trp and $^1O_2$ can be described as shown in Scheme 2a.

Because of the binding of $^1O_2$ to the C3 of Trp, hydrogen of N–H bond is transferred to the O_2^- species to form O–O–H bond at C3 site, which makes the torsion angle about the C_α–C_β–C3=C2 linkage change, and the disappearance of the N–H bending vibration and the changes of fermi double peaks at 1340/1360 cm^{-1}. In addition, the formation of the O–O–H bond changes the electronic density of indole ring and leads to the shifts of some bands related to indole ring, such as the stretching vibration of C=C and the breathing vibration of ring. These changes of bands can be an evidence for the damage of

Table 2
UV resonance Raman bands of Trp in aqueous solution

Raman shift (cm^{-1}) (Trp)	Raman shift (cm^{-1}) (Trp + $^1O_2$)	Assignments[a]
760 (W18)	744 (broadening)	Ring breathing (pyrrole)
1013 (W16)	1027 (broadening)	Ring breathing (benzene)
1340/1360 (W7)	1363 (increase)	Fermi double peak
1466 (W5)	Not observed	δ NH (indole)
1561 (W3)	1585 (decrease)	ν C2=C3 (ring)
1616 (W1)	1616 (increase)	ν C=C (ring)

Band assignments according to Refs. [26,28–30].
[a] Abbreviations: ν, stretching; δ, bending; as, asymmetric modes.

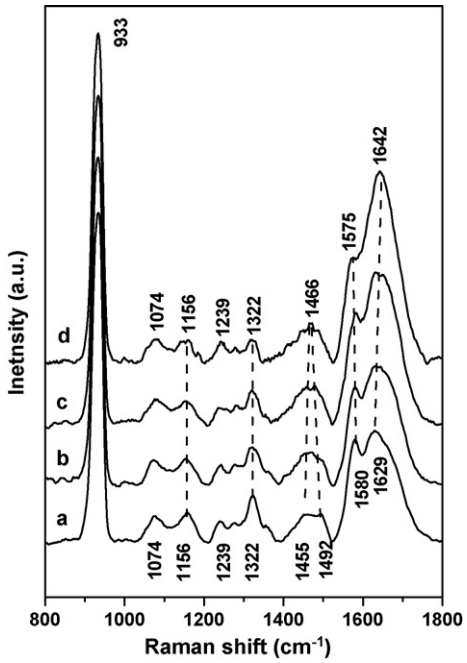

Fig. 3. UV Raman spectra of His at 2.0×10^{-2} M before irradiation (a), after irradiation for 20 min (b), 50 min (c) and 75 min (d) in buffer solution containing 50 mM Tris–HCl, 120 mM $NaClO_4$ (pH 7.5).

Trp and even protein containing Trp motif by $^1O_2$. Reactions of certain amino acids, peptides, and proteins with $^1O_2$ yield the substrate-derived peroxides. Our experimental results indicate that the initial reaction of $^1O_2$ with Trp yields a hydroperoxide at C3. Recent studies have shown that these peroxide species are formed within intact cells and can inactivate key cellular enzymes and even break DNA strands [7,32].

The effect of $^1O_2$ on His was also investigated with UV Raman spectroscopy, as shown in Fig. 3. Raman bands of His are mainly from the imidazole ring and CH_2 group (Table 3). Except for the bands at 1074 and 1239 cm^{-1}, which are corresponding to the skeletal stretching vibration of the side-chain and the C–H in-plane bending vibration of ring, respectively [33,34], other Raman bands of His have some changes after the irradiation. The most significant changes are the decrease of the relative intensity of the band at 1322 cm^{-1}, and the increase of the relative intensity of the band at 1629 cm^{-1} and the shift from 1629 to 1642 cm^{-1}. The band at 1322 cm^{-1} is assigned to the stretching vibrations of the C=N and C–N bonds of imidazole ring and the bend vibration of CH_2 [35,36], and the band at 1629 cm^{-1} is corresponding to the stretching vibrations of both C=C and C=N bonds [35]. The band at 1580 cm^{-1}, ascribed to the stretching vibration of the C=C bond of imidazole ring [34–37], is shifted to 1575 cm^{-1} accompanying a slightly decrease in the intensity. In addition, the relative intensity of the band at 1156 cm^{-1} is also decreased slightly. This band is corresponding to the NH_3^+ rocking and the bending vibration of in-plane NH of imidazole ring [33–36,38]. Two bands at 1455 and 1492 cm^{-1}, ascribed to the ring stretching of imidazole [33,35], are shifted and emerged into one band at 1466 cm^{-1}.

Above results indicate that the reaction of $^1O_2$ with His significantly changes the structure of the imidazole ring, but we failed to confirm the peroxide products that are important intermediates in the photooxidation of His-derived species including the free His and His residues at low temperatures [39]. It was indicated that the detected decay of peroxides is accelerated at the elevated temperatures [6,40]. It is reasonable that peroxides are not main intermediate compounds under our experimental condition, because the solution temperature was increased upon irradiation by a 100 W tungsten lamp. It has been reported that the reaction of $^1O_2$ with Trp can produce the higher peroxide level than that with His, because peroxides formed by His reacting with $^1O_2$ are degraded more rapidly [7]. This report also supports our present results that peroxides were not been detected in the His-$^1O_2$ system under our experimental condition, although we observed the peroxides in the Trp-$^1O_2$ system.

It is worth noting that with increasing irradiation time, the intensity of the band at 1642 cm^{-1} increases remarkably. We speculate that the band at 1642 cm^{-1} comes partially from the stretching vibration of the C=O bond, because the intermediate species decomposed by the initial peroxides contain the C=O bond that comes from the cleavage of the O–O bond [2]. Furthermore, the cleavage of the O–O bond also produces the OH bond that should be close to the CH_2 group, so we observed the evident change of the CH_2 bending vibration.

According to above results, we propose the main species present in the solution after the reaction of His with $^1O_2$ under our experimental condition (Scheme 2b).

Carnosine is a dipeptide consisting of His and β-amino alanine. Fig. 4 shows the UV Raman spectra of the carnosine-porphyrin buffer solution before and after the irradiation. Besides Raman bands of imidazole ring, some amide bands

Table 3
UV Raman bands of His in aqueous solution

Raman shift (cm^{-1}) (His)	Raman shift (cm^{-1}) (His + $^1O_2$)	Assignments[a]
1074	1074	ν C–N (side-chain)
1156	1156 (decrease)	δ NH (in-plane) (ring), NH_3^+ rocking
1239	1239	δ =CH (ring)
1322	1322 (decrease)	ν N=C + ν N–C (ring), δ CH_2
1455	1466	ν ring, δ CH_2
1492	1466	ν ring
1580	1575 (decrease)	ν C=C
1629	1642 (increase)	ν C=C, ν C=N

Band assignments according to Refs. [33–38].

[a] Abbreviations: ν and δ indicate stretching and deformation vibrations, respectively; s, symmetric modes.

Table 4
UV Raman bands of carnosine in aqueous solution

Raman shift (cm^{-1}) (carnosine)	Raman shift (cm^{-1}) (carnosine + $^1O_2$)	Assignments[a]
993	993	CH_2 rock
1100	1100	CH_2 rock
1172	1187 (decrease)	ν N–C–N and δ N–H (ring)
1235	1239	Amide III (ν N–C and δ N–H)
1267	1257 (increase)	Ring breathing
1317	1332 (decrease)	Ring breathing
1373	1373	ν C–N (peptide bond)
1443	1430 (increase)	δ N–H (ring), δ CH_2
1487	1487 (decrease)	δ N–H (ring)
1575	1568	ν C=C
1647	1647	ν C=O amide I

Band assignments according to Refs. [27,33,41–43].
[a] Abbreviations: ν and δ indicate stretching and deformation vibrations, respectively; s, symmetric modes, as, asymmetric modes.

are also observed (Table 4). Compared with His, the intensity and position of the Raman bands of carnosine change dramatically after irradiation in the presence of photosensitizer porphyrin. The band at 1172 cm^{-1} is shifted to 1187 cm^{-1} with the decrease of band intensity, which is ascribed to the N–C–N stretching vibration and NH bending vibration in imidazole ring [26,41–43]. The bands at 1267 and 1317 cm^{-1}, related to the ring breathing vibration of imidazole [39–41], are shifted to 1257 and 1332 cm^{-1}, accompanying the notable increase and decrease of intensity, respectively. The band at 1443 cm^{-1}, corresponding to the NH bend vibration of imidazole ring and the bending vibration of the CH_2 group [27,33,41–43], is shifted to 1430 cm^{-1}, and its relative intensity is increased markedly. On the contrary, the relative intensity of the band at 1487 cm^{-1} is decreased slightly, which is ascribed to the bending vibration of the NH bond of imidazole ring [40,42]. The band at 1575 cm^{-1}, corresponding to the stretching vibrations of the C=C bonds in imidazole ring [27,41–43], is shifted to 1568 cm^{-1}.

No changes in intensity and shift are observed for the bands at 993 and 1100 cm^{-1} ascribed to the CH_2 rocking vibration in the side-chain skeletal [33]. There is a small shoulder peak near the band at 1257 cm^{-1}, and the curve fitting shows that its intensity fails to change but the position is shifted from 1235 to 1239 cm^{-1} that is buried in the band of 1257 cm^{-1} (data not shown). This band at 1235 cm^{-1} is corresponding to amide III. Similarly, the band at 1647 cm^{-1} ascribed to the C=O stretching vibration of amide [41,42] is hardly changed. It was reported that $^1O_2$ does not cause the cleavage of the peptide bond [44], and our result is consistent with this conclusion.

Based on the above results, we can conclude that the damage of $^1O_2$ to carnosine mainly occurs on its imidazole ring, as the ring breathing vibration, the stretching vibration of the C=C bond and the bending vibration of the NH bond in imidazole ring are changed very significantly. In addition, the CH_2 group is also affected by $^1O_2$. The detail damage mechanism induced by $^1O_2$ needs to be studied further.

In addition, we did not find any changes of Raman spectra for His, Trp and carnosine after irradiated for 25, 50, and 75 min in the absence of H_2TMPyP4 (data not shown), this further confirms that their structural damages are due to the effect of $^1O_2$ produced by irradiation of H_2TMPyP4.

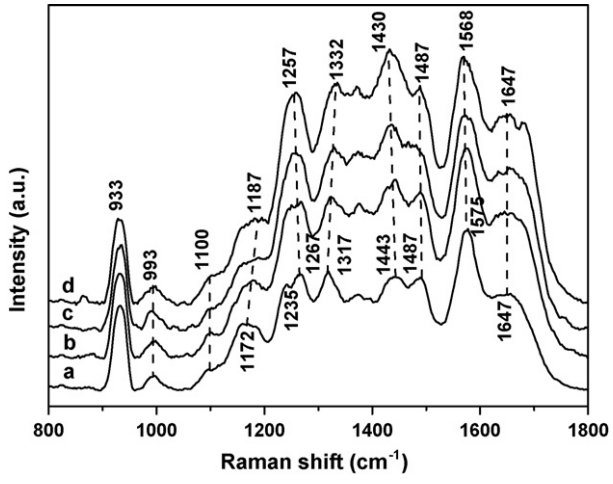

Fig. 4. UV Raman spectra of carnosine at 5.0×10^{-2} M before irradiation (a), after irradiation for 20 min (b), 50 min (c) and 75 min (d) in buffer solution containing 50 mM Tris–HCl, 120 mM $NaClO_4$ (pH 7.5).

4. Conclusions

This study shows that the damage of His, Trp and carnosine by $^1O_2$ can be characterized quantitatively using ATTA-Eu^{3+} complex as a luminescence probe under physiological pH condition. According to the quenching rate constants, carnosine involving His residue is a much more efficient scavenge of $^1O_2$ than His. UV Raman spectroscopy can probe the structural changes of Trp, His and carnosine after their reaction with $^1O_2$. The damage of carnosine by $^1O_2$ occurs mainly in the reaction of its imidazole ring, and the break of the peptide bond is not observed under our experimental condition. The current results provide a new insight into the damage of $^1O_2$ to amino acids and small peptide by the structural change probed by UV Raman and luminescence spectroscopy. In particular, our luminescence probe can be directly applied to measuring the reaction of $^1O_2$ with the biological small molecules.

Acknowledgements

This work was financially supported in part by The National Natural Science Foundation of China (20503029, 20673110) and K.C. Wong Post-doctoral Fellowships (2005).

References

[1] C. Schweitzer, R. Schmidt, Physical mechanisms of generation and deactivation of singlet oxygen, Chem. Rev. 103 (2003) 1685–1757.
[2] M.J. Davies, Singlet oxygen-mediated damage to proteins and its consequences, Biochem. Biophys. Res. Commun. 305 (2003) 761–770.
[3] E. Cló, J.W. Snyder, N.V. Voigt, P.R. Ogilby, K.V. Gothelf, DNA-programmed control of photosensitized singlet oxygen production, J. Am. Chem. Soc. 128 (2006) 4200–4201.
[4] A.M. Edwards, E. Silva, Effect of visible light on selected enzymes, vitamins and amino acids, J. Photochem. Photobiol. B: Biol. 63 (2001) 126–131.
[5] F. Wilkinson, W.P. Helman, A.B. Ross, Rate constants for the decay and reactions of the lowest electronically excited state of molecular oxygen in solution. An expanded and revised compilation, J. Phys. Chem. Ref. Data 24 (1995) 663–1021.
[6] M.J. Davies, Reactive species formed on proteins exposed to singlet oxygen, Photochem. Photobiol. Sci. 3 (2004) 17–25.
[7] E.G. Prestwich, D.R. Marc, J. Rego, S.O. Kelley, Oxidative DNA strand scission induced by peptides, Chem. Biol. 12 (2005) 695–701.
[8] I.B.C. Matheson, R.D. Etheridge, N.R. Kratowich, J. Lee, The quenching of singlet oxygen by amino acids and proteins, Photochem. Photobiol. 21 (1975) 165–171.
[9] R. Kohen, Y. Yamamoto, K.C. Cundy, B.N. Ames, Antioxidant activity of carnosine, homocarnosine, and anserine present in muscle and brain, Proc. Natl. Acad. Sci. U.S.A. 85 (1988) 3175–3179.
[10] T. Keszthelyi, D. Weldon, T.N. Andersen, T.D. Poulsen, K.V. Mikkelsen, P.R. Ogilby, Radiative transitions of singlet oxygen: new tools, new techniques and new interpretations, Photochem. Photobiol. 70 (1999) 531–539.
[11] M.J. Steinbeck, A.U. Khan, M.J. Karnovsky, Extracellular production of singlet oxygen by stimulated macrophages quantified using 9,l0-diphenylanthracene and perylene in a polystyrene film, J. Biol. Chem. 268 (1993) 15649–15654.
[12] B. Song, G. Wang, M. Tan, J. Yuan, Synthesis and time-resolved fluorimentric application of a europium chelate-based phosphorescence probe specific for singlet oxygen, New J. Chem. 29 (2005) 1431–1438.
[13] B. Song, G. Wang, M. Tan, J. Yuan, A new europium chelate-based phosphorescence probe specific for singlet oxygen, Chem. Commun. (2005) 3553–3555.
[14] G. Wang, M. Tan, J. Yuan, A new terbium (III) chelate as an efficient singlet oxygen fluorescence probe, Free Radic. Biol. Med. 40 (2006) 1644–1653.
[15] M. Weng, M.-H. Zhuang, T. Shen, Mercapto-substituted perylenequinonoid pigments. A new type of singlet oxygen sensitizer, Dyes Pigments 36 (1998) 93–102.
[16] A.M. Wade, H.N. Tucker, Antioxidant characteristics of L-histidine, J. Nutr. Biochem. 9 (1998) 308–315.
[17] L.J. Hobart, I. Seibel, G.S. Yeargans, N.W. Seidler, Anti-crosslinking properties of carnosine: significance of histidine, Life Sci. 75 (2004) 1379–1389.
[18] R.H. Bisby, C.G. Morgan, I. Hamblett, A.A. Gorman, Quenching of singlet oxygen by trolox C, ascorbate, and amino acids: effects of pH and temperature, J. Phys. Chem. A 103 (1999) 7454–7459.
[19] B. Song, G. Wang, M. Tan, J. Yuan, A europium (III) complex as an efficient singlet oxygen luminescence probe, J. Am. Chem. Soc. 128 (2006) 13442–13450.
[20] R. Schmidt, Influence of heavy atoms on the deactivation of singlet oxygen ($^1\Delta_g$) in solution, J. Am. Chem. Soc. 111 (1989) 6983–6987.
[21] C.S. Foote, R.W. Denny, Chemistry of singlet oxygen. VII. Quenching by β-carotene, J. Am. Chem. Soc. 90 (1968) 6233–6235.
[22] I.B.C. Matheson, J. Lee, Chemical reaction rates of amino acids with singlet oxygen, Photochem. Photobiol. 29 (1979) 279–881.
[23] J.W. Lee, H. Miyawaki, E.V. Bobst, J.D. Hester, M. Ashraf, A.M. Bobst, Improved functional recovery of ischemic rat hearts due to singlet oxygen scavengers histidine and carnosine, J. Mol. Cell Cardiol. 31 (1999) 113–121.
[24] L. Chinsky, B. Jolles, A. Laigle, P.Y. Turpin, Resonance Raman spectra of poly (L-lysine), aromatic amino acids, L-histidine and native and thermally unfolded ribonuclease A, J. Raman Spectrosc. 16 (1985) 235–240.
[25] Z.Q. Wen, G.J. Thomas Jr., UV resonance Raman spectroscopy of DNA and protein constituents of viruses: assignments and cross sections for excitations at 257, 244, 238, and 229 nm, Biopolymers 45 (1997) 247–256.
[26] S.F. El-Mashtoly, S. Yamauchi, M. Kumauchi, N. Hamada, F. Tokunaga, M. Unno, Structural changes during the photocycle of photoactive yellow protein monitored by ultraviolet resonance Raman spectra of tyrosine and tryptophan, J. Phys. Chem B 109 (2005) 23666–23673.
[27] A. Torreggiani, P. Taddei, G. Fini, Characterization of deoxygenated cobalt (II)-carnosine complexes by Raman and IR spectroscopy, Biopolymers 67 (2002) 70–81.
[28] M. Aki, T. Ogura, K. Shinzawa-Itoh, S. Yoshikawa, T. Kitagawa, A new measurement system for UV resonance Raman spectra of large proteins and its application to cytochrome *c* oxidase, J. Phys. Chem. B 104 (2000) 10765–10774.
[29] H. Takeuchi, Raman structural markers of tryptophan and histidine side chains in proteins, Biopolymers (Biospectroscopy) 72 (2003) 305–317.
[30] T. Miura, H. Takeuchi, I. Harada, Characterization of individual tryptophan side chains in proteins using Raman spectroscopy and hydrogen-deuterium exchange kinetics, Biochemistry 27 (1988) 88–94.
[31] G. Marconi, Theoretical analysis of the resonance Raman spectrum of tryptophan, J. Raman Spectrosc. 22 (1991) 361–365.
[32] A. Wright, W.A. Bubb, C.L. Hawkins, M.J. Davies, Singlet oxygen mediated protein oxidation: Evidence for the formation of reactive side-chain peroxides on tyrosine residues, Photochem. Photobiol. 76 (2002) 35–46.
[33] F.J. Ramírez, I. Tuñón, J.A. Collado, E. Silla, Structural and vibrational study of the tautomerism of histamine free-base in solution, J. Am. Chem. Soc. 125 (2003) 2328–2340.
[34] J.G. Mesu, T. Visser, F. Soulimani, B.M. Weckhuysen, Infrared Raman spectroscopic study of pH-induced structural changes of L-histidine in aqueous environment, Vib. Spectrosc. 39 (2005) 114–125.
[35] A. Torreggiani, M. Tamba, B.G. Fini, Raman and IR study on copper binding of histamine, Biopolymers (Biospectroscopy) 72 (2003) 290–298.
[36] A. Torreggiani, A.D. Esposti, M. Tamba, G. Marconi, G. Fini, Experiemntal and theoretical Raman investigation on interactions of Cu(II) with histamine, J. Raman Spectrosc. 37 (2006) 291–298.
[37] J.G. Mesu, T. Visser, F. Soulimani, E.E. van Faassen, P. de Peinder, A.M. Beale, B.M. Weckhuysen, New insights into the coordination chemistry and molecular structure of copper(II) histidine complexes in aqueous solutions, Inorg. Chem. 45 (2006) 1960–1971.
[38] J.L.B. Faria, F.M. Almeida, O. Pilla, F. Rossi, J.M. Sasaki, F.E.A. Melo, J.M. Filho, P.T.C. Freire, Raman spectra of L-histidine hydrochloride monohydrate crystal, J. Raman Spectrosc. 35 (2004) 242–248.
[39] P. Kang, C.S. Foote, Synthesis of a C-13, N-15 labeled imidazole and characterization of the 2,5-endoperoide and its decomposition, Tetrahedron Lett. 41 (2000) 9623–9626.
[40] V.V. Agon, W.A. Bubb, A. Wright, C.L. Hawkins, M.J. Davies, Sensitizer-mediated photooxidation of histidine residues: Evidence for the formation of reactive side-chain peroxides, Free Radic. Biol. Med. 40 (2006) 698–710.
[41] A. Torreggiani, M. Tamba, G. Fini, Binding of copper(II) to carnosine: Raman and IR spectroscopic study, Biopolymers (Biospectroscopy) 57 (2000) 149–159.
[42] A. Torreggiania, P. Taddeib, A. Tintib, G. Finib, Vibrational study on the cobalt binding mode of carnosine, J. Mol. Struct. 64 (2002) 61–70.
[43] A. Torreggiania, S. Bonora, G. Finib, Raman and IR spectroscopic investigation of zinc(II)-carnosine complexes, Biopolymers (Biospectroscopy) 57 (2002) 352–364.
[44] M. Tomita, M. Irie, T. Ukita, Sensitized photooxidation of histidine and its derivatives. Products and mechanism of the reaction, Biochemistry 8 (1969) 5149–5160.